

Approximate Heat Transfer Solution for the Breed and Burn Molten Salt Reactor

Alisha Kasam, Eugene Shwageraus

Department of Engineering, University of Cambridge, Cambridge CB2 1PZ, United Kingdom
aak52@cam.ac.uk, es607@cam.ac.uk

Abstract - A proposed breed-and-burn molten salt reactor (BBMSR) concept uses separate fuel and coolant salts, with fuel salt contained in tubes similar to conventional solid fuels. Natural convection of the molten fuel within the tubes aids heat transfer to the coolant, allowing larger fuel diameters than with solid fuel. The thermal-hydraulic design of such a core layout normally requires computationally intensive modelling of natural convection in the fuel. This paper introduces a method for efficient thermal-hydraulic analysis of this molten salt configuration. A heat transfer correlation is derived to estimate the "effective" conductivity, which incorporates the effects of heat transfer by both natural convection and conduction in the fuel. CFD simulations for a single fuel tube are performed with varying parameters to determine the relationship between the maximum fuel temperature and parameters such as fuel salt properties, tube diameter, and power density. The CFD results are used to calibrate the coefficients of the effective thermal conductivity correlation. Maximum fuel salt temperature estimates by the correlation method can be generated quickly and show excellent agreement with the CFD results.

I. INTRODUCTION

A breed-and-burn molten salt reactor (BBMSR) with separate fuel and coolant salt is proposed to meet the Generation IV objectives of improved fuel sustainability, waste management, and proliferation resistance. The BBMSR is a novel reactor concept that combines the advantages of breed-and-burn (B&B) and molten salt reactor (MSR) technologies while avoiding the primary disadvantages of each. MSRs allow high temperature operation at atmospheric pressures, flexible fuel cycle operation, and inherent safety due to strongly negative reactivity feedback. A BBMSR configuration using two separate salts is based on the design of the Stable Salt Reactor (SSR) by Moltex Energy LLP. The SSR is a fast-spectrum plutonium burner that contains a fuel-carrying molten salt in individual fuel tubes, which can be periodically replaced like in LWRs [1]. Natural convection of the molten fuel within the tubes aids heat transfer to the coolant, while physical separation of the fuel and coolant has numerous neutronic and materials advantages. Fig. 1 shows a side view of the SSR core layout, where the fuel assemblies are submerged in a clean coolant salt circulated by forced convection.

The fuel tubes concept allows for improved neutron economy and simplified reactor design compared to a traditional single-fluid MSR. The absence of fuel in the external reactor circuit avoids the drift of delayed neutron precursors. In traditional MSRs, the production of delayed neutrons outside the core results in loss of reactivity, requirement for shielding of the external circuit, and neutronic sensitivity to pump speed. Confinement of fuel to assemblies at the centre of the core also reduces the required mass of fissile and fertile material, as well as corrosion and irradiation damage to the pumps and reactor vessel.

While the extent of corrosion in the fuel cladding depends on numerous factors, the ease of replacement of assemblies is a key feature that should allow high operating temperatures and neutron fluence in the fuel. Fuel element fabrication is greatly simplified for a molten salt compared to solid fuels,

and the liquid fuel can be easily transferred to fresh cladding and reinserted into the core to achieve the burnup needed for B&B operation. With the BBMSR, high uranium utilisation can be realised in a simple, passively safe reactor with minimal waste generation and proliferation risk.

Molten salt reactors can achieve high power densities and thermodynamic efficiencies due to the high operating temperatures of the fuel and coolant. In the two-salt geometry, low thermal resistance at the cladding interface enhances heat transfer to the coolant, and natural convection of the fluid inside the container allows fuel temperature limits to be maintained at a higher power rating than with conduction alone [3]. Still, adequate heat transfer from fuel salt to coolant must be ensured to avoid fuel boiling and cladding failure. B&B operation in general requires high fuel loading and a very hard spectrum, which can be achieved for the BBMSR by using pure UCl_3 fuel salt, large fuel tube diameter, and chloride salt coolant. However, the tube diameter is limited by the efficiency of heat transfer from the fuel, and the UCl_3 concentration may be

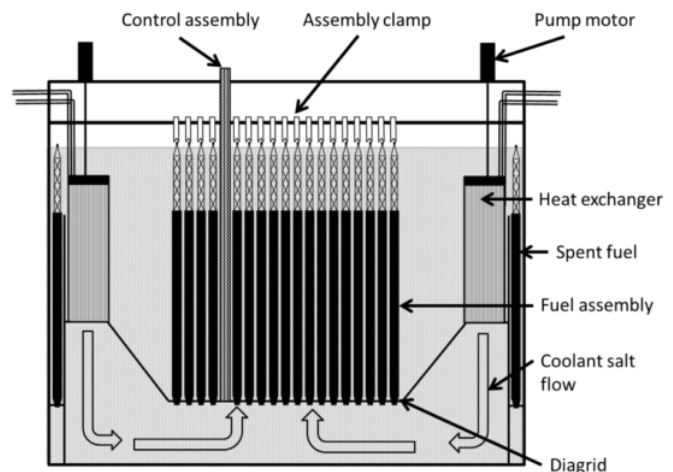


Fig. 1: SSR side view [2]

limited by its high melting temperature, nearly 850°C for the pure salt [4]. Low-enriched fuel, containing less than 20% ^{235}U , may enable B&B operation with a mixture of UCl_3 and carrier salt NaCl in the fuel.

In this work, we investigate the influence of tube diameter, UCl_3 concentration (affecting the thermophysical properties of the fuel), and power density on the thermal–hydraulic performance of the BBMSR fuel tube. With solid fuel, simple radial conduction heat transfer calculations can be used to relate the fuel power density to fuel, cladding, and coolant temperatures. With the two-salt fuel tube configuration, a detailed understanding of natural convection in a heat-generating fluid is required for modelling and optimisation of the BBMSR. The velocity and temperature distributions are coupled, so the mass, momentum, and energy equations must be solved simultaneously. Section II. presents these equations and reviews two approaches from literature for analysing natural convection of a liquid fuel in a vertical cylinder. Section III. describes the development of a computational fluid dynamic (CFD) model for estimating the heat transfer from a single long vertical tube of molten salt fuel to coolant. Section IV. introduces a novel approach for approximating natural convection effects in the fuel tube. The approximate solution can be used to efficiently explore the design space of the BBMSR, Moltex SSR, and any other reactor with a similar liquid-fuel configuration.

II. NATURAL CONVECTION MODELLING

In this section, the Navier–Stokes equations are presented and simplified for the case of the vertical molten salt fuel tube. An analytical solution to the equations and a recent CFD study of the system of interest are reviewed and compared.

1. Navier–Stokes Equations

Convection in a molten salt fuel tube can be mathematically modelled as a constant-property flow with internal heat generation and isothermal walls. The Navier–Stokes equations include the mass and momentum continuity equations, which solve the flow part of the convection problem, and the energy conservation equation, which solves the heat transfer part of the problem. The constant-property approximation of the Navier–Stokes equations is sufficiently accurate for convective flows in which the temperature variations are small relative to the absolute temperature of the fluid [5]. The convective flow of molten salt fuel is assumed to fulfil the constant-property criterion, and so is treated as incompressible and constant-property. In the vertical cylinder analysed as a two-dimensional system, x is the radial distance from the vertical axis, and y is the distance from the lower end of the cylinder.

A. Mass

The continuity of mass principle requires that for an incompressible fluid,

$$\frac{\partial u}{\partial x} + \frac{\partial v}{\partial y} = 0 \quad (1)$$

where u and v are the local velocity components at (x, y) .

B. Momentum

The momentum equations are derived from the Navier–Stokes equations describing the motion of a fluid in terms of force balances. The x -momentum equation is given by

$$\rho \left(u \frac{\partial u}{\partial x} + v \frac{\partial u}{\partial y} \right) = -\frac{\partial p}{\partial x} + \mu \left(\frac{\partial^2 u}{\partial x^2} + \frac{\partial^2 u}{\partial y^2} \right) \quad (2)$$

where ρ is the fluid density, p is the pressure, and μ is the laminar viscosity. The y -momentum equation is similar, with an added term for the body force from g , acceleration due to gravity.

$$\rho \left(u \frac{\partial v}{\partial x} + v \frac{\partial v}{\partial y} \right) = -\frac{\partial p}{\partial y} + \mu \left(\frac{\partial^2 v}{\partial x^2} + \frac{\partial^2 v}{\partial y^2} \right) - \rho g \quad (3)$$

C. Energy

The energy equation is derived from the First Law of Thermodynamics requiring a balance of energy in the control volume. For an incompressible fluid with constant thermal diffusivity α and uniform volumetric heat generation rate \dot{q} , the distribution of temperature T is given by [5]

$$u \frac{\partial T}{\partial x} + v \frac{\partial T}{\partial y} = \alpha \left(\frac{\partial^2 T}{\partial x^2} + \frac{\partial^2 T}{\partial y^2} \right) + \dot{q} \quad (4)$$

D. Boussinesq Approximation for Buoyancy

The temperature and flow fields of the convection problem are coupled via the fluid equation of state, which is approximated as

$$\rho \approx \rho_S [1 - \beta(T - T_S)] \quad (5)$$

where ρ_S and T_S are the density and temperature at the geometry surface, ρ is the lower local density, and T is the warmer local temperature. β is the coefficient of thermal expansion at constant pressure,

$$\beta = -\frac{1}{\rho} \left(\frac{\partial \rho}{\partial T} \right)_p \quad (6)$$

The Boussinesq approximation can be used for buoyancy-driven flow in an incompressible fluid [5]. By the constant-property approximation, variations in density are small enough to have a negligible effect on the formulas except where density is multiplied by g . The inertial difference due to the effect of gravity on fluids of different densities is incorporated into the Navier–Stokes equations as a buoyancy term. In Equation 3, the pressure gradient $\partial p/\partial y$ can be reduced to $dp_0/dy = -\rho_0 g$, and Equation 5 is substituted into the body force term of Equation 3. The resulting Boussinesq-approximated y -momentum equation is

$$\rho \frac{\partial v}{\partial x} + v \frac{\partial v}{\partial y} = \nu \frac{\partial^2 v}{\partial x^2} + g\beta(T - T_S) \quad (7)$$

where g , β , T_S , and the kinematic viscosity $\nu = \mu\rho_S^{-1}$ can be assumed constant. In Equation 4, α is calculated as

$$\alpha = \kappa(\rho_S c)^{-1} \quad (8)$$

where the thermal conductivity κ and specific heat c are also assumed constant.

2. Analytical Solution From Literature

Martin used the Buoyant Boussinesq-approximated Navier–Stokes equations to predict convective heat transfer of a heat-generating fluid in a long vertical cylinder [3]. Previous analysis and experimental studies of convection in heat-generating fluids show that the hot core rises while the cooler annulus falls [6, 7]. The radial velocity and temperature profiles were assumed to be as shown in Fig. 2. In short cells, the annulus grows from the bottom to the top, while in cells of large length-to-radius ratio, the end effects become relatively unimportant and the annulus evolves to a constant thickness [3].

The axial temperature gradient depends on the distribution of the volumetric heat source, and on the external thermal boundary conditions due to the coolant flow. For the isothermal wall case, the axial temperature gradient tends towards maxima at the ends and minima at mid-length. The maximum temperature occurs at the top of the cylinder when closed-end gradients are neglected. Martin derived a closed-form solution for the case of Prandtl number $Pr = \infty$, when the axial velocity

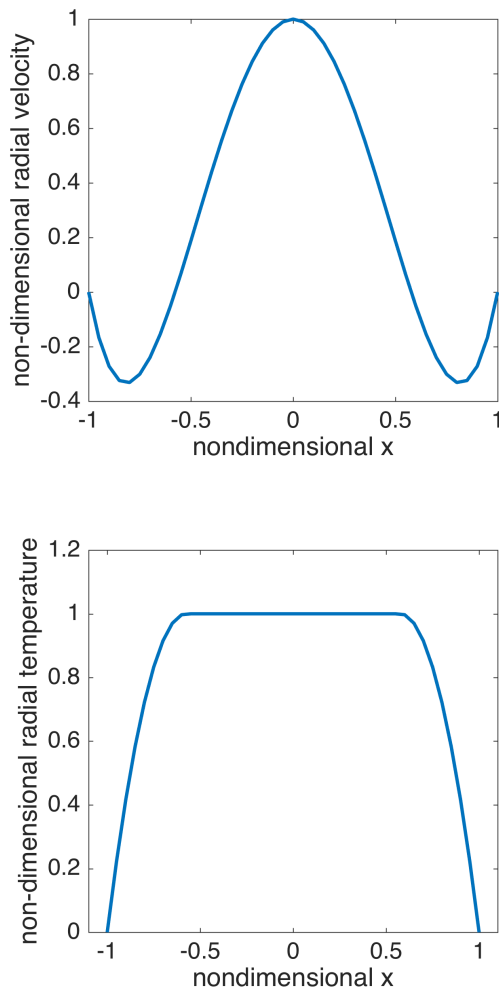


Fig. 2: Assumed radial velocity and temperature profiles in natural convection [3]

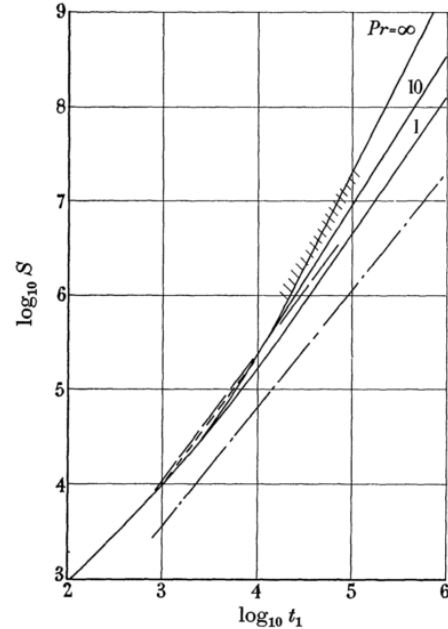


Fig. 3: Analytically predicted relation between heat generation rate and temperature on axis at top of cylinder [3]

is linearly proportional to the axial temperature [3].

For finite Pr , a general closed-form solution cannot be found due to the interdependence of velocity and temperature. The nonlinear relationship between axial temperature and velocity was instead described by a truncated polynomial series, where the coefficients are evaluated for the specific value of the dimensionless heat generation rate S ,

$$S = \dot{q}\beta gr^6(\nu\alpha kL)^{-1} \quad (9)$$

and the dimensionless fluid temperature at the top of the cylinder t_1

$$t_1 = \beta gr^4(T_1 - T_S)(\nu\alpha L)^{-1} \quad (10)$$

where r is the cylinder radius, L is the length, T_1 is the fluid temperature at the top of the cylinder, and T_S is the wall temperature. Fig. 3 displays the predicted relationships between S and t_1 for $Pr = 1$, $Pr = 10$, and $Pr = \infty$. Experimental measurements from various other studies are indicated by the dashed lines up to $t_1 < 10^{4.8}$, showing good agreement with Martin's analytical solution; it was hypothesised that a transition to turbulence occurs beyond this temperature. The predicted relationships suggested that heat transfer occurs mainly by conduction for $t_1 < 10^3$, while convective heat transfer dominates above this threshold.

3. Computational Solution From Literature

Leefe, et al. used ANSYS Fluent software to perform computational fluid dynamic (CFD) calculations to show that the Moltex fuel tube design is feasible [8]. A tube of 1.5 m height was modelled with fuel salt NaCl/UCI₃/PuCl₃ (60/20/20 mole %) and coolant salt KF/ZrF₄/NaF (48/42/10

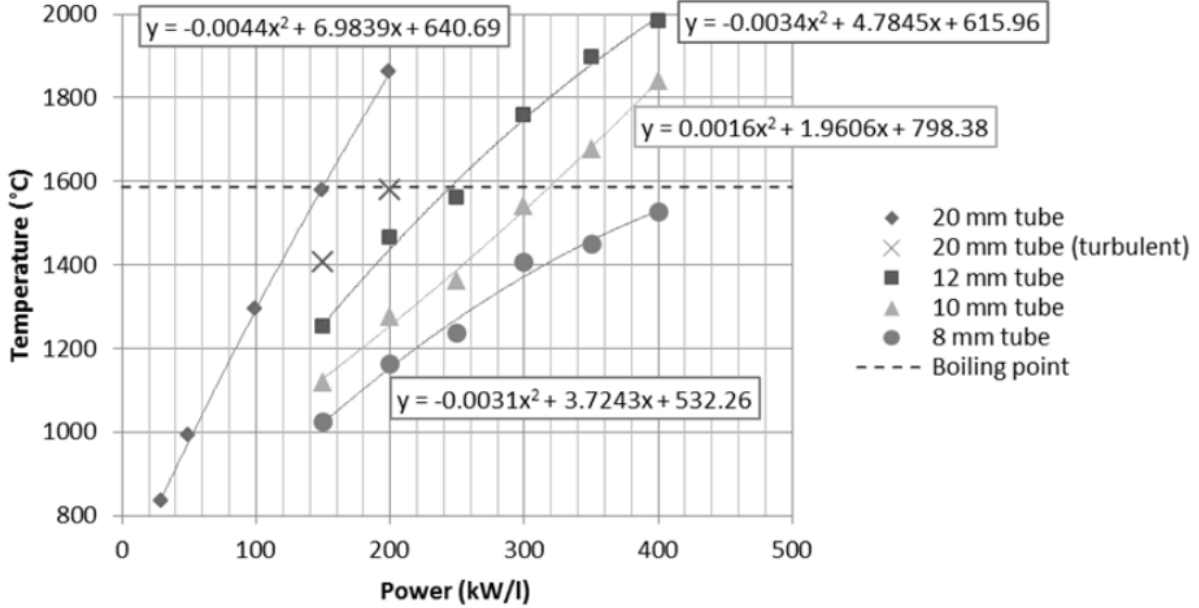


Fig. 4: Maximum fuel salt temperature from prior CFD study [8]

mole %). Based on the fission heat generation rate, the maximum temperature was calculated for fuel salt, tube wall, and coolant salt at different tube diameters and power densities. The assumptions used in the study are not given, but it is inferred that a constant wall heat flux condition was used in order to determine the influence on the cladding and coolant temperatures. Laminar flow was simulated for diameters between 8 mm and 20 mm, with the results shown in Fig. 4.

At diameters smaller than 8 mm, steady state conditions cannot be established due to drag on the tube walls. The 20 mm simulation indicated a transition to turbulence, so a turbulent solution was also produced for this diameter. From the results it was concluded that for 10 mm diameter tubes, 250 kW per liter of fuel salt is achievable while remaining 200°C below the fuel boiling point. The cladding and coolant temperatures remain well within the safe margins of operation due to the highly efficient heat transfer from molten salt fuel to coolant.

4. Comparison of Methods from Literature

Next, we compare the analytical solution from [3] with the CFD results from [8] in order to evaluate the degree of similarity between the two solutions. The fuel salt modelled in [8] (properties given in Table II) has been used as the reference fuel. Equation 9 is used to calculate the dimensionless heat generation rate S for each data point in Fig. 4, the plot from the CFD study. Fig. 3 is then used to estimate the predicted dimensionless temperature t_1 . However, the divergence of the $S - t_1$ relationship for $Pr = 1$ and $Pr = 10$ when $S > 10^{4.5}$ introduces some difficulty, since the Prandtl number of the molten fuel

$$Pr = \nu/\alpha \quad (11)$$

TABLE I: Maximum difference between CFD and analytical solution of maximum fuel temperature

Diameter (mm)	Error (%)
8	10.45
10	9.44
12	6.79
20	32.32

ranges from 9.74 at 500°C to 3.57 at 1000°C. The $Pr = 10$ relation on Fig. 3 has ultimately been used to estimate t_1 , and the maximum fluid temperature T_1 is then calculated according to Equation 10.

The maximum temperatures predicted by Martin's analysis are plotted on Fig. 5 together with the fitted curves from the prior CFD study. Using the CFD results as the reference solution, the error of the analytical result has been determined for each estimated value. Table I gives the maximum error for each tube diameter over the power densities calculated. The methods show relatively good agreement for the 8, 10, and 12 mm cases, but for the 20 mm case the analytical method predicts up to 32% lower temperatures than the CFD model. This can be explained partly because Pr is closer to 1 than 10 at the temperatures estimated by the CFD model for the 20 mm tube. In addition, it was noted previously that flow in the 20 mm tube may be in the laminar-turbulent transition regime, but Martin's analytical solution has only been verified experimentally for laminar flow.

III. CFD MODEL FOR THE BBMSR

The analytically predicted $S - t_1$ relationship is shown to have limited validity for molten salt fuel convection at the

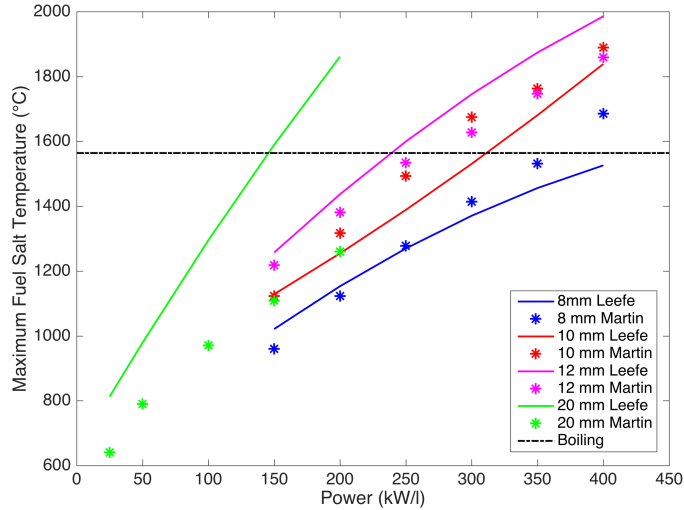


Fig. 5: Comparison of CFD method [8] and analytical Navier–Stokes solution [3] for estimating maximum fuel salt temperature

larger diameters that may be of interest for the BBMSR. Thus, a computational approach has been selected for analysis of convection in the BBMSR fuel tube.

1. OpenFOAM Model Description

An OpenFOAM solver is written for a heat-generating fluid in a vertical cylinder with an isothermal wall boundary condition. OpenFOAM is an open-source C++ library that can be used to solve continuum mechanics problems and manipulate data via solvers and utilities [9]. It has been extensively used for CFD modelling, and its flexibility makes it a convenient tool for solving the unusual heat transfer problem of a heat-generating molten salt in a cooled, vertical cylinder.

The OpenFOAM model is based on the existing *buoyantBoussinesqSimpleFoam* solver, described as a "steady-state solver for buoyant, turbulent flow of incompressible fluids" [9]. The solver iteratively solves the Buoyant Boussinesq-approximated Navier–Stokes equations to produce velocity and temperature profiles for the given geometry, fluid properties, and boundary conditions. The user supplies the geometry mesh and the fluid properties.

To model natural convection in the molten salt fuel, a custom version of the solver is written with addition of a heat source term in the temperature equation. The finite element meshing software Gmsh is used to generate a semi-unstructured grid, where the top circular surface of the fuel tube is unstructured while the extruded length of the tube is structured, as shown in Fig. 6. Either an initial reference temperature or a temperature boundary condition is required. The OpenFOAM temperature boundary condition *externalWallHeatFluxTemperature* is used to simulate the isothermal tube walls. The bulk coolant temperature and coolant heat transfer coefficient are defined by the user to represent the isothermal case. The coolant thermal conductivity is also incorporated into the boundary condition to calculate total heat transfer.

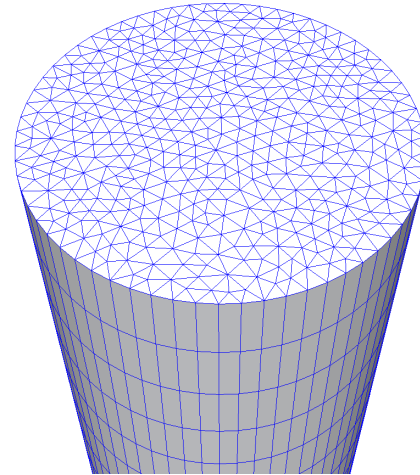


Fig. 6: Unstructured mesh from Gmsh

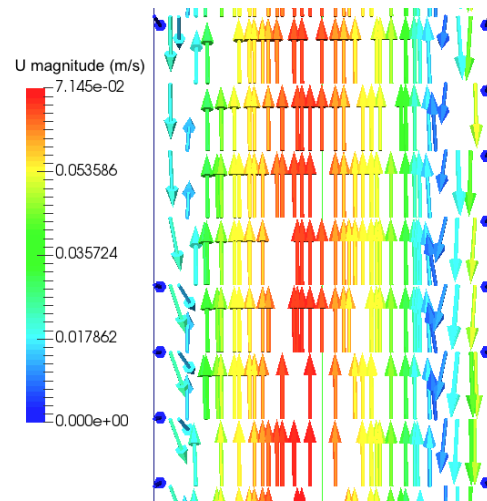


Fig. 7: OpenFOAM solution of fuel salt velocity distribution

2. Model Verification

The temperature and velocity profiles produced by the OpenFOAM model agree with those described in the literature. Fig. 7 shows the solution with a rising core and falling annulus.

For quantitative verification of the OpenFOAM model, the geometry and fuel salt modelled in the prior CFD study – described in Part 3. of Section II – are used as a reference case. The values of ρ , c , and kinematic viscosity ν are evaluated at 850°C (1123 K) according to the fuel salt's thermophysical properties given in [8]. The fuel thermal conductivity κ and coolant temperature T_{∞} for the temperature boundary condition are also taken from the prior CFD study. Equations 5 and 11 are used to calculate β and Pr , respectively. An isothermal wall with coolant heat transfer coefficient h_{cool} equal to $34\text{ kW} \cdot \text{m}^{-2}\text{K}^{-1}$ is used to define the temperature boundary condition. Table II summarises the OpenFOAM inputs for this model verification setup.

The OpenFOAM model is used to simulate each combination of tube diameter and power density shown on Fig. 4. In order to model the small diameters simulated in the prior

TABLE II: Molten salt fuel properties for CFD model verification

	Reference Fuel Specifications [8]	OpenFOAM Model Inputs (Properties Evaluated at 850°C)
Composition	NaCl/UCl ₃ /PuCl ₃ (60/20/20 mole %)	
Boiling point	1837 K	
Density, ρ	$4.1690 - (9.014 \times 10^{-4}T[\text{K}]) \text{ kg} \cdot \text{m}^{-3}$	$3021.5 \text{ kg} \cdot \text{m}^{-3}$
Kinematic viscosity, ν	$\exp(-1.2675 + 1704/T[\text{K}])10^{-6} \text{ m}^2\text{s}^{-1}$	$1.2839 \times 10^{-6} \text{ m}^2\text{s}^{-1}$
Thermal conductivity, κ	$0.5 \text{ W} \cdot (\text{m} \cdot \text{K})^{-1}$	$0.5 \text{ W} \cdot (\text{m} \cdot \text{K})^{-1}$
Specific heat capacity, c	$520 \text{ J} \cdot (\text{kg} \cdot \text{K})^{-1}$ at 730 K to $670 \text{ J} \cdot (\text{kg} \cdot \text{K})^{-1}$ at 1837 K	$550 \text{ J} \cdot (\text{kg} \cdot \text{K})^{-1}$
Coolant temperature, T_∞	450°C	
Prandtl number, Pr	4.458	
Coefficient of thermal expansion, β	$2.5628 \times 10^{-4} \text{ K}^{-1}$	
Coolant heat transfer coefficient, h_{cool}	$34 \text{ kW} \cdot \text{m}^{-2}\text{K}^{-1}$	

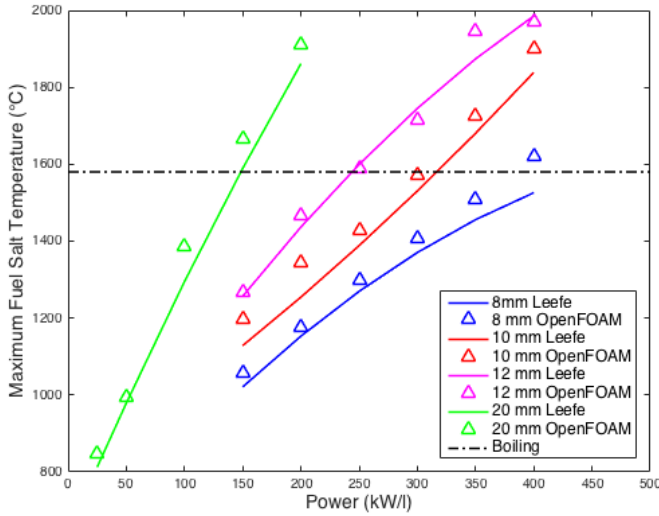


Fig. 8: Maximum fuel salt temperature from Leefe [8] and OpenFOAM results

CFD analysis, the default turbulent flow option in the buoyantBoussinesqSimpleFoam solver is switched off. Fig. 8 compares the results from the OpenFOAM molten salt convection model with the fitted curves from the prior study (Fig. 4). The results show good agreement, with less than 10% error for all calculated points, even though the OpenFOAM model uses an isothermal wall whereas the prior study uses the constant wall heat flux condition. The accuracy of an isoflux wall boundary condition will be investigated in the future.

Each fuel tube simulation in OpenFOAM takes approximately 4 hours to converge on a 2.60 GHz CPU. While the CFD model provides useful detail into the velocity and temperature distributions in a single fuel element, scaling up to larger and more complex systems could become prohibitive in terms of time and computational resources.

IV. EFFECTIVE CONDUCTIVITY DESCRIPTION AND RESULTS

The present study aims to develop a heat transfer correlation that incorporates the effects of both radial conduction and vertical convection in the BBMSR fuel. The correlation can be used to find an approximate heat transfer solution from simple algebraic conduction equations. This section describes the steps taken to define and calibrate the correlation, which will enable efficient thermal-hydraulic analysis for fuel assembly and core design of the BBMSR.

1. Defining a Heat Transfer Correlation

For a fuel element at steady state conditions, the heat generated within the fuel must equal the heat convected from the external surface to the moving coolant. A liquid fuel transfers heat to its internal surface by both conduction and convection in the fuel material. To simplify the heat transfer analysis, we define an effective conductivity κ_{eff} of a representative stationary fluid, which transfers the same amount of heat as the actual moving fluid.

Assuming heat conduction in the radial direction only and constant κ_{eff} , the cylindrical form of the heat equation is

$$\frac{1}{r} \frac{d}{dr} \left(r \frac{dT}{dr} \right) + \frac{\dot{q}}{\kappa_{eff}} = 0 \quad (12)$$

With symmetry, the maximum temperature is found at the centreline. The temperature distribution is solved by integrating Equation 12 twice, assuming symmetrical boundary conditions and constant thermal conductivity. The centreline temperature T_0 can then be found if the surface temperature T_S is known, where r_0 is the fuel radius:

$$T_0 - T_S = \frac{\dot{q}r_0^2}{4\kappa_{eff}} \quad (13)$$

T_S can be related to the ambient or bulk coolant temperature T_∞ by an energy balance using the coolant's convective heat transfer coefficient h_{cool} :

$$T_S - T_\infty = \frac{\dot{q}r_0}{2h_{cool}} \quad (14)$$

Next, κ_{eff} must be defined such that both conduction and convection effects are accounted for. This can be written in terms of the Nusselt number, Nu , a dimensionless parameter which equals the ratio of convection to pure conduction heat transfer.

$$\kappa_{eff} = Nu \cdot \kappa \quad (15)$$

Typically, Nu for a specific geometry, fluid, and type of flow is calculated using an empirical correlation, with coefficients determined from experimental data. The heat transfer coefficient h_{hot} of the flow in a cylinder of diameter D can then be calculated as:

$$h_{hot} = \frac{Nu \cdot \kappa}{D} \quad (16)$$

A Nu correlation for the system with heat-generating, naturally convecting fluid in a vertical cylinder has not been found in the literature. To develop such a correlation for use in thermal-hydraulic analysis of the BBMSR, we assume it to take the algebraic form of a correlation provided for natural convection heat transfer between two concentric cylinders or spheres [11],

$$\frac{\kappa_{eff}}{\kappa} = a \left(\frac{Pr}{b + Pr} \right)^m Ra^n \quad (17)$$

where the coefficients a , b , m , and n are empirically determined from experimental data, and the Rayleigh number Ra , is a dimensionless parameter used to characterise buoyancy-driven flow. Ra is defined for a vertical cylinder as

$$Ra = \frac{g\beta(T_0 - T_S) D^3}{\nu\alpha} \quad (18)$$

and the properties β , ν , and α are evaluated at the film temperature, $T_{film} = T_0 + T_S$ [12]. Equation 18 is substituted into Equation 17 to produce the heat transfer correlation:

$$\frac{\kappa_{eff}}{\kappa} = a \left(\frac{Pr}{b + Pr} \right)^m \left(\frac{g\beta(T_0 - T_S) S^3}{\nu\alpha} \right)^n \quad (19)$$

Rearranging and inserting Equation 19 into Equation 13, the centreline temperature T_0 can be solved for:

$$(T_0 - T_S)^{1+n} = \frac{\dot{q}r_0^2}{4a \left(\frac{Pr}{b+Pr} \right)^m \left(\frac{g\beta S^3}{\nu\alpha} \right)^n \kappa} \quad (20)$$

$$T_0 = \left[\frac{\dot{q}r_0^2}{4a \left(\frac{Pr}{b+Pr} \right)^m \left(\frac{g\beta S^3}{\nu\alpha} \right)^n \kappa} \right]^{1/(1+n)} + T_S \quad (21)$$

In the absence of experimental data to calibrate the values of a , b , m , and n , the OpenFOAM CFD model described in Section III. can be used to generate a set of simulated temperature data.

TABLE III: Density and viscosity in the UCl_3 -NaCl system

UCl_3 mole %	c	d	A_v	$B_v \times 10^3$
100	6.3747	1.5222	1.2213	1.1000
85	5.5847	1.0869	1.7723	1.7865
60	4.8964	1.0470	1.7404	1.7190
40	4.1966	0.9072	1.6404	1.5640
33	3.8604	0.8371	1.5715	1.4647

TABLE IV: OpenFOAM Model Inputs

OpenFOAM Model Inputs	
Thermal conductivity, κ	0.7 W · (m · K) ⁻¹ [14]
Specific heat capacity, c	435.60 J · (kg · K) ⁻¹ [15]
Coolant temperature, T_∞	827°C
Film temperature, T_{film}	1455°C
Coolant heat transfer coeff., h_{cool}	34 kW · m ⁻² K ⁻¹

2. Simulating Results Using CFD

The OpenFOAM CFD model is used to calculate the maximum fuel salt temperature for a range of tube diameters, power densities, and salt concentrations. The tube diameters 10, 15, 20, 30, and 50 mm and power densities 100, 150, 200, 250, 300, 350, and 400 kW/l have been analysed in neutronic feasibility studies of the BBMSR, so they are also included in this study to represent a design space of interest. The thermophysical properties for a range of UCl_3 -NaCl mixtures have been determined experimentally by Desyatnik, et al. [13]. The mixtures containing 100, 85, 60, 40, and 33 mole % are simulated in this study, using the density and viscosity properties given in Table III. The density ρ is calculated from the coefficients c and d as

$$\rho = [c - (d \cdot 10^{-3})T_{film}] \times 10^3 \quad (22)$$

The viscosity ν is calculated from A_v and B_v as

$$\nu = 10^{-A_v+B_v/T_{film}} \times 10^{-6} \quad (23)$$

Equations 8, 5, and 11 are respectively used to calculate α , β , and Pr . Table IV gives the values of OpenFOAM inputs assumed for all combinations; thermal conductivity and specific heat data for UCl_3 -NaCl mixtures were not found in the literature, so values for pure UCl_3 have been carried through. Turbulent operation is assumed for all cases, so the turbulent version of the solver has been used. In total, 175 combinations of tube diameter, power density, and mole % UCl_3 are simulated in OpenFOAM to cover this design space.

3. Heat transfer correlation fit

The set of 175 maximum fuel temperatures from all cases is used for fitting the coefficients of the effective conductivity correlation. MATLAB's linear regression feature is used to find the values of a , b , m , and n . Table V shows the results of this fit, including the 95% confidence intervals of each coefficient. When this model is used to estimate T_0 for all 175 cases,

TABLE V: Coefficients of Equation 21

Coefficient	95% confidence bounds	
a	0.2338	(0.1328, 0.3349)
b	0.3146 E-3	(-1.213, 1.213)
m	358.3	(-1.38 E 6, 1.381 E 6)
n	0.2454	(0.2359, 0.2548)

TABLE VI: Coefficients of Equation 25

Coefficient	95% confidence bounds	
a	0.06851	(0.062, 0.07503)
m	0.08055	(0.04855, 0.1125)
n	0.2938	(0.2895, 0.2981)

the maximum error compared to the CFD results is 7.71%. It can be seen that b and m both have confidence bounds that are orders of magnitude greater than the values themselves, indicating that these two coefficients may be correlated and can be combined into a single coefficient operating on Pr .

Equation 21 is rewritten to a slightly modified form, omitting the denominator of the Pr term to produce a correlation of the form

$$\frac{\kappa_{eff}}{\kappa} = a \cdot Pr^m \cdot Ra^n \quad (24)$$

The approximate solution to T_0 is then

$$T_0 = \left[\frac{\dot{q}r_0^2}{4a \cdot Pr^m \left(\frac{g\beta S^3}{\nu\alpha} \right)^n \kappa} \right]^{1/(1+n)} + T_S \quad (25)$$

Table VI shows the results of the fit for the modified correlation, which produces a maximum error of 4.61% compared to the CFD results. The calibration step takes less than 5 seconds in MATLAB, and the recalculation of the entire set of 175 results using the correlation model takes less than 1 second, in comparison to the 4 hours required to simulate a single point in CFD.

Figs. 9 and 10 show the maximum temperature T_0 and effective conductivity κ_{eff} results obtained from CFD and from the approximate solution using the developed correlation. The effective conductivity κ_{eff} was calculated for the CFD results by comparing the maximum temperature of the simulated convecting fuel with that predicted by a pure conduction solution according to Equation 13. The influences of power density and tube diameter on heat transfer behaviour can be clearly observed, while the sensitivity to UCl_3 concentration is small. Figs. 11 and 12, showing the temperature results for the 100 mole % UCl_3 fuel salt with varying diameter and power density configurations, provide a snapshot of the trends.

The validity of the coefficients given in Table VI is limited to the range of tube sizes, power densities, and salt mixtures modelled. However, the approach can be easily applied to a new set of cases, for example if a new salt composition is considered for the reactor concept. Only a small number of CFD points would need to be generated at the boundaries of the range to calibrate the correlation coefficients. The effective

conductivity correlation could then be used to interpolate for the maximum fuel temperature at any point within the range.

The correlation presented here could be validated with experimental results, but this is outside the scope of this work. The approximate heat transfer solution could also potentially be improved by optimising the form of the correlation expression. Nusselt number correlations take numerous forms for different geometries and flow orientations, and a detailed comparison of these forms and their suitability to the fuel tubes case could be undertaken. In this study, a simple form has been assumed and found to be sufficiently accurate for the purposes of BBMSR fuel tube design. The confidence bounds of m in Table VI are still moderately large, but as the bounds are the same order of magnitude as the coefficient value, the fit is considered adequate.

V. SUMMARY AND CONCLUSIONS

MSRs have several neutronic, thermal hydraulic, and fuel cycle advantages over solid-fuelled fast reactor configurations. The BBMSR incorporates the Moltex SSR fuel tube design, which isolates the molten salt fuel in tube assemblies. The fuel tube concept enables improved neutron economy, simplified reactor design, and periodic replacement of fuel elements to realise the high burnups needed for B&B operation.

Enhanced heat transfer by natural circulation of the salt inside the tube allows larger tube diameters than with solid fuels, so the core can contain a higher fuel volume fraction. Natural convection in heat-generating fluid is a complex flow scenario on which limited studies have been published. In the present work, an OpenFOAM CFD model has been developed for a single fuel tube with an isothermal surface. Even for this simplified system, around 700 CPU hours are required to model the design space consisting of 7 power densities, 5 salt concentrations, and 5 tube diameters.

A novel approach to approximate the heat transfer solution of liquid fuel tubes has been introduced as a tool to efficiently search the design space. Using the approximate fuel temperature distribution, the methods that are well established for solid-fuelled reactors can be applied to construct detailed thermal-hydraulic models, easily incorporating effects such as cladding thermal resistance and coolant convection between fuel elements.

The coefficients of the effective conductivity correlation derived in this work are calibrated with a set of 175 results from the OpenFOAM CFD model. The calibration step requires less than 5 seconds to complete. The set of results is recalculated from the correlation model, taking less than 1 second and producing a maximum error of less than 5%. In future work, the form of the correlation can be optimised to improve its calculation accuracy or expand its validity to more design variants, and even to include radiation heat transfer in the semi-transparent molten salt fuel. However, the model and its coefficients presented in this paper are sufficient for the current stage of development of the BBMSR concept, and produce significant time savings compared to the CFD approach.

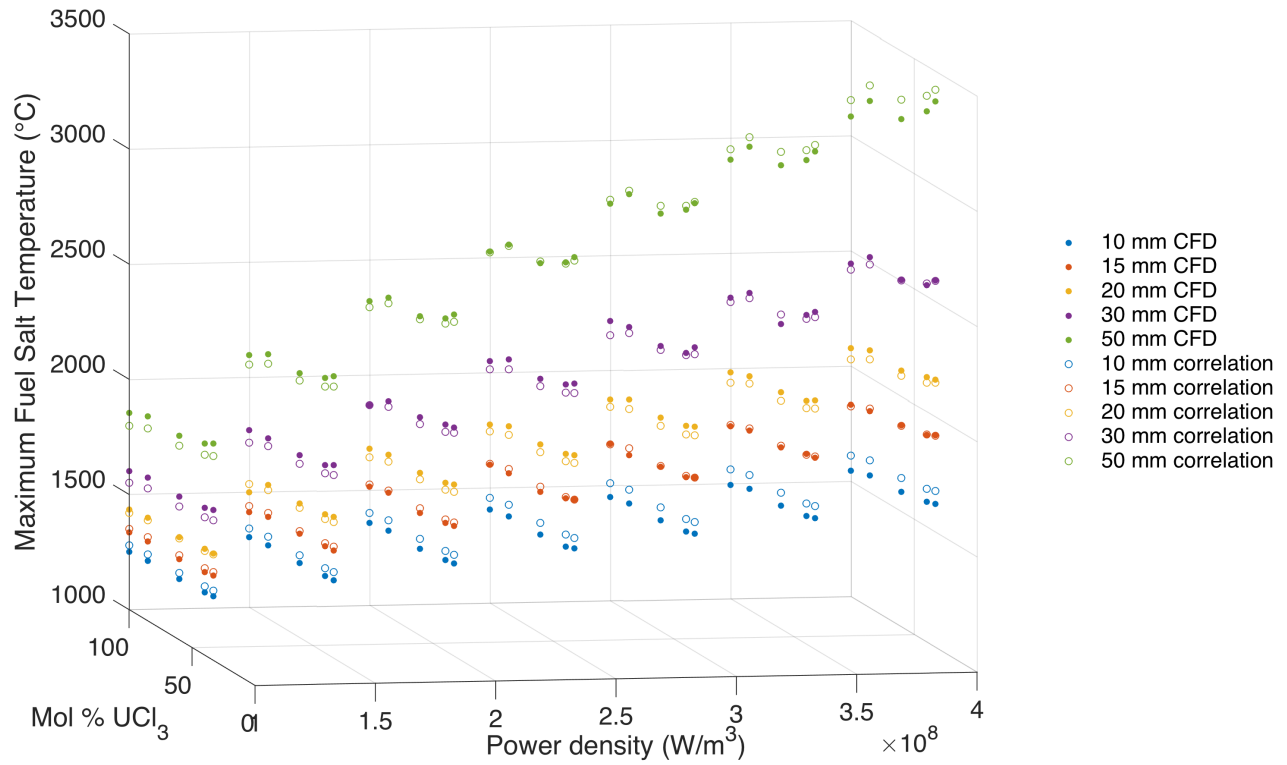


Fig. 9: Maximum fuel temperature: comparison of results from CFD and developed heat transfer correlation

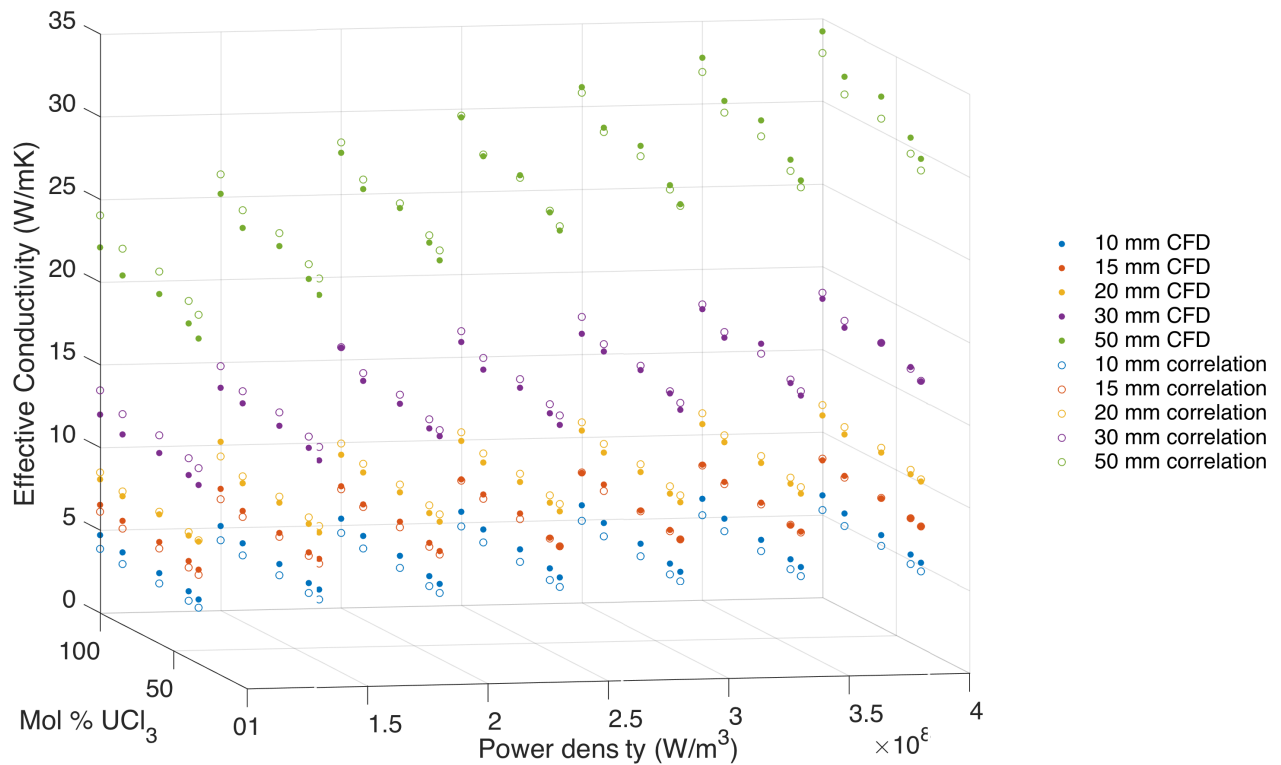


Fig. 10: Effective conductivity: comparison of results from CFD and developed heat transfer correlation

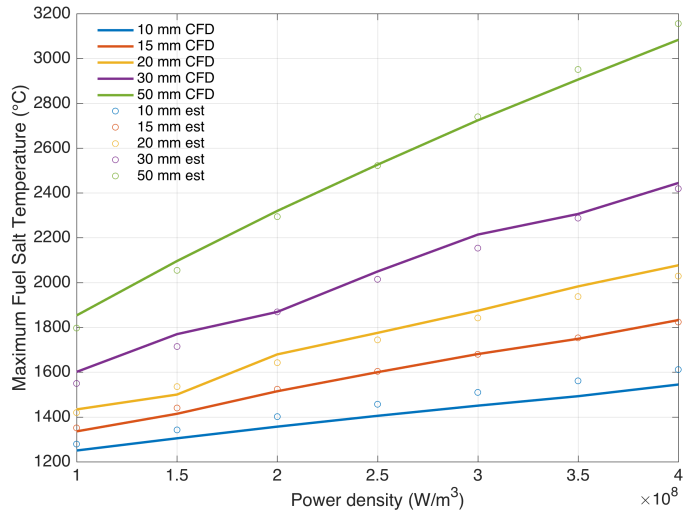


Fig. 11: Maximum fuel temperature versus power density for different tube diameters and 100 mole % UCl_3

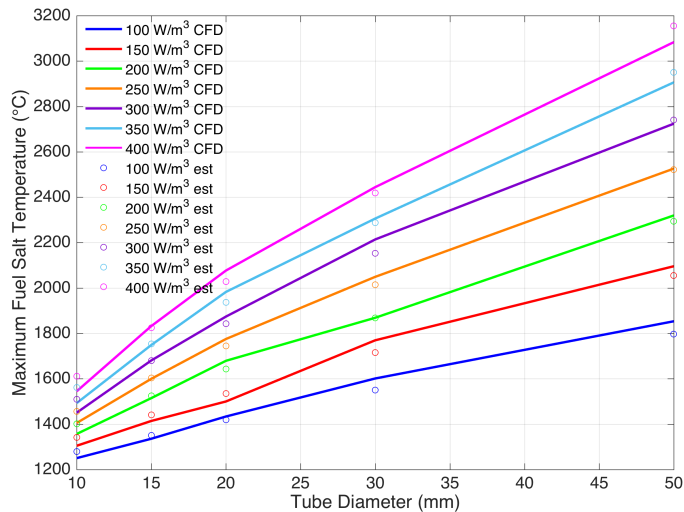


Fig. 12: Maximum fuel temperature versus tube diameter for different power densities and 100 mole % UCl_3

VI. ACKNOWLEDGMENTS

The authors thank Xinyu Zhao for guidance with OpenFOAM modelling, and the first author gratefully acknowledges the Cambridge Trust for PhD funding.

REFERENCES

1. I. SCOTT, "Gaseous and Volatile Fission Produce Release From Molten Salt Nuclear Fuel," in "Proceedings of the Thorium Energy Conference," Mumbai, India (2015).
2. I. SCOTT, T. ABRAM, and O. NEGRI, "Stable Salt Reactor Design Concept," in "Proceedings of the Thorium Energy Conference," Mumbai, India (2015).
3. B. MARTIN, "Free convection in a vertical cylinder with internal heat generation," *Proceedings of the Royal Society of London*, **301**, 327–341 (1967).
4. R. E. THOMA, "Phase diagrams of nuclear reactor materials," Tech. rep., Oak Ridge National Laboratory (1959).
5. A. BEJAN, *Convection Heat Transfer*, John Wiley & Sons, Inc., second ed. (1995).
6. M. V. JOSHI, U. N. GAITONDE, and S. K. MITRA, "Analytical Study of Natural Convection in a Cavity With Volumetric Heat Generation," *Journal of Heat Transfer*, **128**, 2, 176 (2006).
7. A. SIAHPUSH and J. CREPEAU, "Scale Analysis of Convective Melting with Internal Heat Generation," in "Proceedings of the ASME/JSME 2011 8th Thermal Engineering Joint Conference," ASME, Honolulu, Hawaii, USA (2011), pp. 1–7.
8. S. LEEFE, P. JACKSON-LAVER, and I. R. SCOTT, "Computation Fluid Dynamic Modelling of Natural Convection Heat Flow in Unpumped Molten Salt Fuel Tubes," in "Proceedings of the Thorium Energy Conference," Mumbai, India (2015).
9. C. J. GREENSHIELDS, "OpenFOAM 3.0.1 User Guide," (2015).
10. S. GLASSTONE and A. SESONSKE, *Nuclear Reactor Engineering*, Van Nostrand Reinhold Company, third ed. (1981).
11. G. RAITHBY and K. HOLLANDS, *A General Method of Obtaining Approximate Solutions to Laminar and Turbulent Free Convection Problems*, vol. 11, Academic Press, New York (1975).
12. F. P. INCROPERA, D. P. DEWITT, T. L. BERGMAN, and A. S. LAVINE, *Fundamentals of Heat and Mass Transfer*, John Wiley & Sons, Inc., sixth ed. (2007).
13. V. DESYATNIK, S. KATYSHEV, S. RASPOPIN, and Y. F. CHERVINSKII, "Density, Surface Tension, and Viscosity of Uranium Trichloride-Sodium Chloride Melts," *Atomnaya Energiya*, **39**, 1, 70–72 (jul 1975).
14. M. TAUBE, "Fast Reactors Using Molten Chloride Salts as Fuel," Tech. rep., Swiss Federal Institute for Reactor Research (1978).
15. O. BENEŠ and R. J. M. KONINGS, "Thermodynamic evaluation of the $\text{NaCl-MgCl}_2\text{-UCl}_3\text{-PuCl}_3$ system," *Journal of Nuclear Materials*, **375**, 2, 202–208 (2008).